PHYSICAL REVIEW E VOLUME 58, NUMBER 4 OCTOBER 1998

Shear-induced micellar crystal structures in an aqueous triblock copolymer solution

T. M. Slawecki, C. J. Glinka, and B. Hammouda
National Institute of Standards and Technology, Gaithersburg, Maryland 20899
(Received 20 January 1998)

Shear-induced structures have been observed in aqueous solutions of the triblock copolymer $PEO_{25}PPO_{40}PEO_{25}$ in the micellar crystalline region of the temperature-concentration phase diagram. A structure induced by steady shear, having two-dimensional (2D) hexagonal symmetry over macroscopic dimensions, transforms reversibly to a crystalline structure with different symmetry upon cessation of shear. Other structures are induced with oscillatory shear, including a 3D hexagonal phase with Bragg peaks that not only persist but sharpen with the cessation of shear. Over the range of temperature, concentration, and shear conditions investigated, no evidence for cubic or cubatic crystalline phases has been observed.
[S1063-651X(98)50110-9]

PACS number(s): 61.25.Hq, 61.12.Ex, 83.50.Ax, 83.70.Hq

I. INTRODUCTION

The phase behavior of aqueous solutions of amphiphilic triblock copolymers has been of great interest recently [1–3]. In particular, triblocks of polyethylene oxide (PEO) and polypropylene oxide (PPO) have been found to possess rich structure in solution due to the increasing hydrophobicity of PPO with increasing temperature [3–7]. Known commercially as ''Pluronics'' (BASF Corp.) or ''Poloxamers'' (ICI), $PEO_nPPO_mPEO_n$ triblocks are soluble in water at low temperatures, but are driven to aggregate and form micelles as the temperature is raised. Further heating at certain concentrations leads to a polycrystalline gel phase, which can be aligned to form a single crystal by imposing a small shear field [8].

This Rapid Communication focuses on previously unreported shear-induced structures in aqueous solutions of $PEO_{25}PPO_{40}PEO_{25}$. Numerous studies have already been conducted on this ''Pluronic'' [3,9,10]. Most notably, Mortensen and co-workers have mapped its phase behavior and report the presence of a cubatic body-centered cubic (BCC) spherical micelle phase, a hexagonal rodlike micellar phase, and lamellar phases attainable at higher concentrations and temperatures [3]. In a similar experiment, Diat and co-workers deduced the existence of a highly twinned face-centered cubic (FCC) structure in a very different Pluronic (F108) subjected to laminar shear using x-ray scattering [11]. They were the first to publish scattering patterns obtained from two orthogonal views (see Fig. 1, top) of a pluronic crystal and also reported oscillatory shear-induced FCC twins, each occupying one half of the shear cell gap, resulting in two distinct sets of tangentially observed Bragg spots.

In the present work, SANS is used to reveal the steady and oscillatory shear-induced patterns in $PEO_{25}PPO_{40}PEO_{25}$. We report for the first time the relaxation of a shear-induced crystal structure to a different crystalline phase upon cessation of steady shear. We also report several crystal patterns resulting from oscillatory shear depending upon solution concentration and magnitude and frequency of shear, one giving rise to strong, narrow Bragg peaks like those speculated to arise only in Pluronics with larger PEO blocks [3].

II. EXPERIMENTAL DETAILS AND RESULTS

$PEO_{25}PPO_{40}PEO_{25}$ (Pluronic P85, BASF Corporation, Parsippany, NJ) was dissolved in D_2O at 5 °C to make 25 and 30 wt. % solutions. D_2O was used to provide good contrast with the P85 in SANS experiments. Fully dissolved solutions were studied in 0.5 and 1 mm gap Couette-type shear cells consisting of a 59 or 60 mm diameter inner cylindrical quartz stator and a 61 mm diameter outer quartz rotor. Thermostating fluid circulating through the interior of the stator and through a thermal housing exterior to the rotor provided good temperature control and eliminated concerns about thermal gradients across the sample. A nylon cap covering the shear cell stator and rotor inhibited solvent evaporation.

Experiments were conducted on both the NG3 and NG7 30 m SANS instruments at the National Institute of Standards and Technology, configured with a neutron wavelength of $\lambda = 0.5$ nm ($\Delta\lambda/\lambda = 0.1$) and sample-to-detector distances of 2.55 to 4.25 m. Translation of the shear cell stage in the beam permitted access to both radial and tangential views of the sample undergoing shear, as depicted at the top of Fig. 1. A 1.27 cm diameter circular aperture was used in radial geometry while a 0.5 mm×1.27 cm slit was used for all tangential geometry measurements.

Samples of 25 wt. % solution were heated slowly from 5 °C to 30 °C to permit complete formation of spherical micelles. Under static conditions, at 35 °C, the SANS ring pattern, indicative of the spherical micelle spacing, became speckled due to the formation of polycrystallites. At $T = 40$ °C, well into the reported micellar BCC region, the sample was subjected to steady shear at 20 s^{-1}. Figure 1(a) shows prominent sixfold symmetric primary and secondary diffraction spots when viewed radially and ''modulated tube'' features [12] when viewed tangentially. The sixfold radial pattern is consistent with the radial SANS patterns reported by Mortensen [3,9], and both patterns are, surprisingly, quite similar to those reported by Diat and co-workers for the pluronic F108 [11]. Thus, it is not readily apparent whether the 20 s^{-1} structure is BCC, FCC, or something else.

Based upon previous reports of P85 behavior, it was expected that the 20 s^{-1} structure would remain intact upon

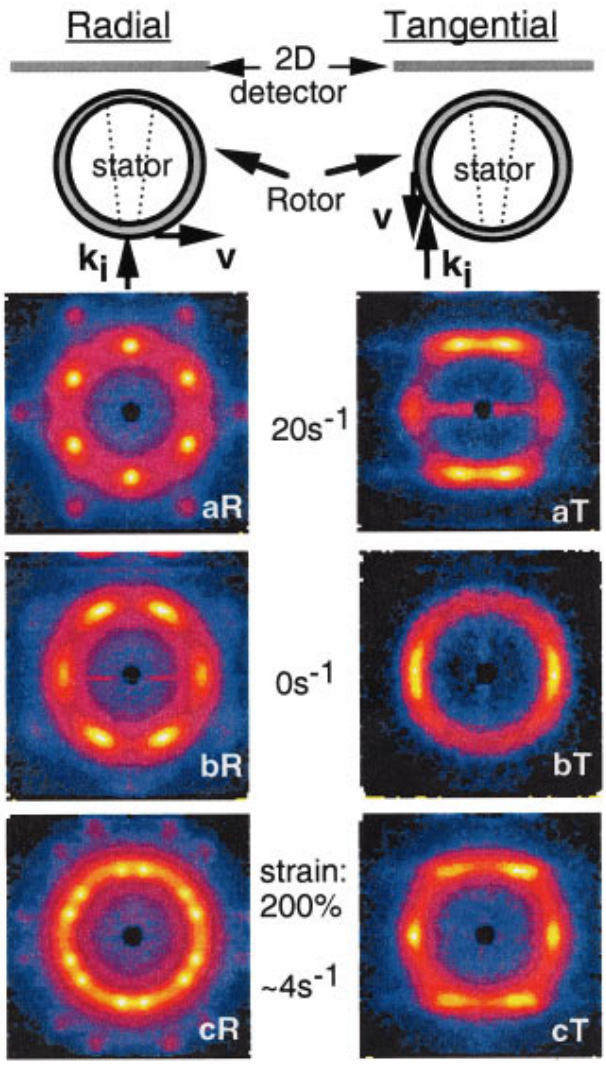

FIG. 1. (Color) Radial (R) and tangential (T) SANS patterns observed in 25 wt. % P85 in D_2O under steady shear (a), cessation of shear (b), and oscillatory shear (c). At the top is a schematic of a top view of the shear cell with the sample-filled cell gap marked in gray. The flow direction, $\mathbf{v}$, is indicated; the shear gradient, ∇, points radially inward, and the vorticity axis e points out of the page. In radial geometry, the incident beam, $k_i \| \nabla$ and $k_i \perp \mathbf{v}$; in tangential geometry, $k_i \| \mathbf{v}$ and $k_i \perp \nabla$ ($0.1\,\mathrm{nm}^{-1} \leqslant Q \leqslant 1.0\,\mathrm{nm}^{-1}$). Ghost reflections at the top of (bR) and the thin (one channel) horizontal line across its middle are artifacts of the detector. The Couette shear cell gap was 0.5 mm.

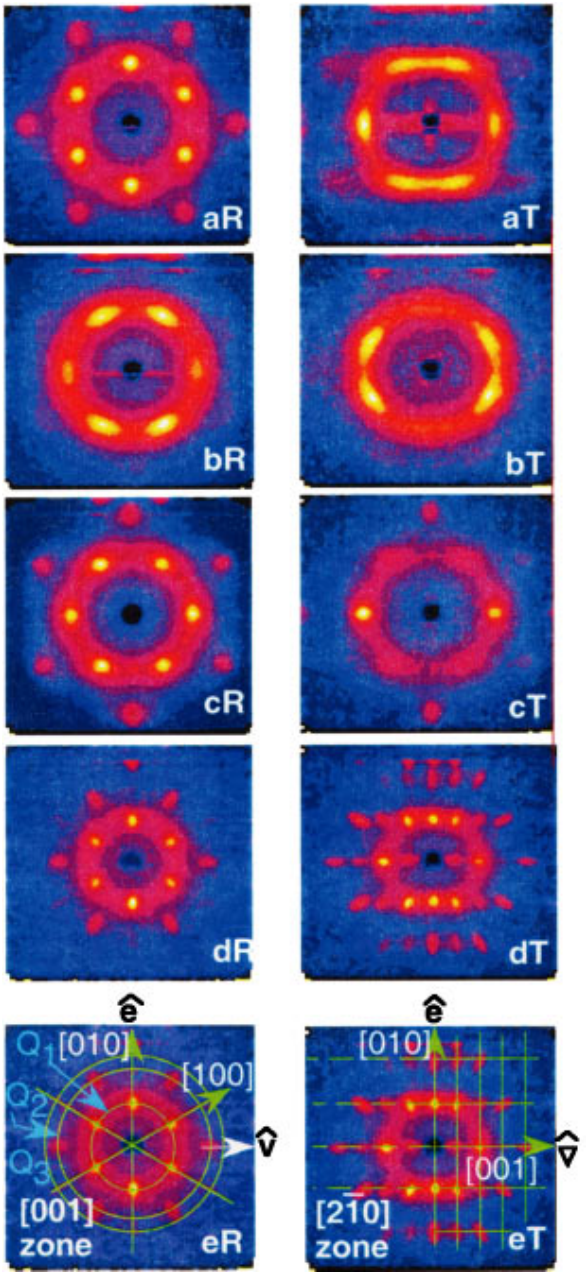

FIG. 2. (Color) Radial (R) and tangential (T) SANS patterns observed in 30 wt. % P85 in D_2O (a) during 20 s^{-1} steady shear, (b) 2 h *after cessation of* steady shear, (c) *after cessation of* a gentle applied oscillatory shear at 200% strain and $\approx 8\,s^{-1}$ maximum shear, and (d) *after cessation of* a strong applied oscillatory shear at 400% strain and $\approx 17\,s^{-1}$ maximum shear. (e) Hexagonal indexing of the patterns in (d). $0.1\,\mathrm{nm}^{-1} \leqslant Q \leqslant 1.0\,\mathrm{nm}^{-1}$, except for (d) and (e) for which $0.2\,\mathrm{nm}^{-1} \leqslant Q \leqslant 1.6\,\mathrm{nm}^{-1}$ to exhibit higher ordered features. Ghost reflections at the top of the SANS images are an artifact of the detector. The Couette shear cell gap was 1 mm.

removal of shear. Unexpectedly, cessation of shear [Fig. 1(b)] altered the SANS pattern within 100 s. The radial geometry pattern retains six strong primary peaks, but they are no longer of equal intensity nor exactly 60° apart, and the pattern is rotated. Even more striking is the static tangential view, Fig. 1(bT), which is markedly different from that observed at 20 s^{-1} [Fig. 1(aT)]. Once formed, the static patterns did not alter further with time, but would always transform reversibly to those of Fig. 1(a) with the reimposition of 20 s^{-1} steady shear. A smaller applied shear (e.g., 5 s^{-1}), created the same patterns as those observed at 20 s^{-1}, but the Bragg spots were more smeared along the annulus, in agreement with what others have reported [8]. Nevertheless, at 0 s^{-1}, the sample clearly relaxed to a different crystal structure observable in both the 0.5 and 1 mm gap Couette cells; hence there was not a ''gap effect'' [13].

The only way found to retain a shear-induced structure was to impose oscillatory shear on the sample. The SANS patterns shown in Fig. 1(c) (200% strain, 4 s^{-1}) appear to be identical to those in Fig. 1(a) except that every peak is now split. Each pair of peaks sits $\pm 10°$ relative to the unsplit [Fig. 1(a)] peak positions. Even the less well-defined peaks

in the tangential pattern appear to broaden and split when subjected to oscillatory shear. Because this splitting is observed in *both* geometries, the structure formed is different from that observed by Diat and coworkers, as discussed previously. Equally striking is the persistence of this pattern upon removal of shear: it was still present 20 min after the oscillatory shear was *stopped*, at which point the pattern was finally disrupted by imposing a steady shear, again reproducing the patterns in Fig. 1(a).

It was found that repeated application and removal of shear over a period of hours gradually lessened the ability of the spherical micelles to form crystallites in any capacity in the 25 wt. % solution. Changing temperature in either direction failed to restore polycrystallinity once it was lost. In contrast, the spherical micelles which formed in the 30 wt. % solution were found to be more durable and continued to align reproducibly under shear over the course of several days.

The 30 wt. % solution was heated similarly to that of the 25 wt. % and exhibited polycrystallinity by 25 °C; thus, the patterns displayed in Fig. 2 were obtained at 30 °C. As was observed at 25 wt. %, the $20\ s^{-1}$ steady-shear pattern [Fig. 2(a)] relaxed to a different structure upon removal of shear [Fig. 2(b)]; however, the kinetics were much slower: approximately two hours at $0\ s^{-1}$ was required to completely form this pattern. More interestingly, the *tangential* view of this static crystal structure is slightly different from what was observed previously in Fig. 1(b), suggesting the evolution of order that was incipient at 25 wt. %.

A gentle applied oscillatory shear (200% strain, $8\ s^{-1}$) was found to generate a pattern that resembled a more well-defined $0\ s^{-1}$ pattern but with a significantly altered tangential pattern. Following 45 min of oscillatory shear, this pattern sharpened even more when shearing was *stopped* [Fig. 2(c)]. A similar behavior was observed *after* subjecting the sample to a stronger oscillatory shear (400% strain, $17\ s^{-1}$) for 20 min, as seen in Fig. 2(d). This latter pattern resembles that of the steady shear pattern of Fig. 2(a) except that the peaks are now sharply defined and are smeared only by the instrumental resolution. It is further remarkable to observe peaks out to third order both radially and tangentially in these types of systems. Similar to the 25 wt. % solution, these oscillatory shear-induced patterns exhibited no tendency to change significantly on the timescale of hours and were disrupted only by imposing a steady shear. Hybrid structures were observed at other oscillatory shear settings, possessing the combined features of Figs. 2(c) and 2(d).

III. DISCUSSION

Various crystal structures, in both cubic and hexagonal space groups, were investigated in attempting to account for the diffraction peak positions shown in Figs. 1 and 2. The ratio of the the Q values of the second to first order peaks (Q_2/Q_1) measured for the patterns obtained in *radial* geometry do not correspond to known crystallographic ratios except for the case of the highly aligned structure of Fig. 2(dR), for which $Q_2/Q_1=\sqrt{3.00}$. In fact, for the faint third order peaks in Fig. 2(dR), $Q_3/Q_1=1.96$, essentially $\sqrt{4}$. These ratios hold true for both cubic and hexagonal arrangements and thus the radially-observed pattern alone is insufficient for determining the structure.

It was only in the case of the well-localized patterns generated by strong oscillatory shear, Fig. 2(d), that a structure was found which accounted for *all* observed peak locations in *both* radial *and* tangential geometries. The ratios of the Q values of the peaks along the vertical (vorticity, $\mathbf{e}$) axis to the innermost peak along the horizontal (shear gradient, ∇) axis were measured to be: $Q_{1,\mathbf{e}}/Q_{1,\nabla}=1.82$; $Q_{2,\mathbf{e}}/Q_{1,\nabla}=3.65$. Only a hexagonal unit cell (space group P6/mmm) of dimensions $a=b=13.3$ nm and $c=20.9$ nm satisfies these radial *and* tangential reciprocal space ratios [see Fig. 2(e)]. The basal plane dimensions are in good agreement with the micellar ''hard-sphere'' size of ≈ 6.0 nm, as measured on samples under static (unsheared) conditions using the fitting methods outlined elsewhere [3]. The ratio $c/a=1.57$ is close to that for a hard sphere hexagonal close-packed (HCP) structure (1.63); however, if the structure were HCP, there would be no intensity at the $(00l)$ reciprocal lattice points for odd l, whereas weak peaks are observed at (001) and (003). [see Fig. 2(eT)].

The SANS patterns observed under $20\ s^{-1}$ steady shear [Figs. 1(a) and 2(a)] are obviously closely related to the simple hexagonal structure described above. The tangential views of Figs. 1(aT) and 2(aT) are indicative of a loss of long-range translational order in the direction of the shear gradient, but there is much less corresponding loss of order in the radial views. We have been able to generate patterns based on random registered stacking of hexagonal close-packed planes of spherical micelles, with the nearest neighbor spacing in the flow direction, that qualitatively resemble those observed in both the radial and tangential geometries. Hence, the structure of the flowing system appears to consist of highly oriented close-packed planes parallel to the shear cell walls, that move relative to one another with a slip-stick type of motion among the interstitial sites in adjacent planes. This type of structure and motion has been observed in a number of concentrated ''hard'' and ''soft'' sphere systems [14,11], but not yet in P85.

Upon cessation of shear, contrary to ''hard'' and ''soft'' sphere behavior, the P85 steady shear-induced structure was *not* retained indefinitely, nor did the crystal ''melt'' to its previous polycrystalline state. Rather, both the $0\ s^{-1}$ ''relaxed'' pattern [Figs. 1(b) and 2(b)] to which it transforms and the gentle [Fig. 2(c)] oscillatory shear-induced patterns are unique and are *not* simply rotated versions of the $20\ s^{-1}$ or hexagonal crystal structures, as demonstrated by the patterns observed tangentially. No suitable monodomain or twinned cubic arrangement of spherical micelles was found to fit *any* of these remaining patterns. In the case of the split-peak pattern of Fig. 1(c), the possibility of rotated crystals is being explored. Micellar deformation under shear is an unlikely cause of these unexplained patterns since the solution is at rest in one case and under gentle shear in the other, whereas the strongest (oscillatory) shear generated nearly perfect 3D arrangement of undeformed spheres [Fig. 2(d)]. Extending theoretical models of diblocks [15,16] to triblock behavior holds promise for better understanding these solutions.

IV. CONCLUSIONS

The scattering patterns observed in 25 and 30 wt. % aqueous solutions of the P85 triblock copolymer appear to be truly shear-induced and not simply the result of shear alignment of polycrystalline domains as evidenced by (a) changes in the patterns as a function of magnitude and frequency of oscillatory shear, and (b) the reversible ''relaxation'' of the steady shear-induced structure to a crystalline structure having different symmetry. The latter behavior is a new and surprising result that we suspect is specific to this type of self-assembled colloidal system and contrasts sharply with what has been observed in other (whether ''hard'' or ''soft'') spherical particle systems.

Two orthogonal views of the sample were found to be important to deduce the underlying crystal structures and to distinguish them from the very similar cubic and cubatic crystal patterns of which we found no evidence. In general, the reproducibility and durability of the shear-induced structures depends upon location in the phase diagram. Thus, the 30 wt. % solutions exhibited slower kinetics and more well-defined, durable patterns than those observed at 25 wt. %; the latter is closer to the micellar liquid boundary making it more likely to be affected by shear-induced melting of the crystals. We continue to investigate why these micellar arrangements arise and which is the true equilibrium structure.

ACKNOWLEDGMENTS

This work is based on activities supported by the National Science Foundation under Grant No. DMR-9122444. We appreciate useful discussions with F. S. Bates, K. Almdal, and P. Alexandridis.

[1] P. Alexandridis and T. A. Hatton, Colloids Surf., A **96**, 1 (1995).
[2] P. Alexandridis, J. F. Holzwarth, and T. A. Hatton, Macromolecules **27**, 2414 (1994).
[3] K. Mortensen, J. Phys.: Condens. Matter **8**, A103 (1996), and references therein.
[4] G. Wanka, H. Hoffman, and W. Ulbricht, Macromolecules **27**, 4145 (1994).
[5] R. K. Prud'homme, G. Wu, and D. K. Schneider, Langmuir **12**, 4651 (1996).
[6] P. Linse and M. Malmsten, Macromolecules **25**, 5434 (1992).
[7] P. Alexandridis, D. Zhou, and A. Khan, Langmuir **12**, 2690 (1996).
[8] K. Mortensen, W. Brown, and B. Norden, Phys. Rev. Lett. **68**, 2340 (1992).
[9] K. Mortensen, Europhys. Lett. **19**, 599 (1992).
[10] J. S. Pedersen and M. C. Gernstenberg, Macromolecules **29**, 1363 (1996).
[11] O. Diat, G. Porte, and J.-F. Berret, Phys. Rev. B **54**, 14 869 (1996).
[12] B. J. Ackerson and N. A. Clark, Phys. Rev. A **30**, 906 (1984).
[13] B. Hammouda, J. Mang, and S. Kumar, Phys. Rev. E **51**, 6282 (1995).
[14] B. J. Ackerson, J. B. Hayter, N. A. Clark, and L. Cotter, J. Chem. Phys. **84**, 2344 (1986); S. E. Paulin, B. J. Ackerson, and M. S. Wolfe, Phys. Rev. E **55**, 5812 (1997).
[15] S. Qi and Z.-G. Wang, Macromolecules **30**, 4491 (1997).
[16] G. A. McConnell, M. Y. Lin, and A. P. Gast, Macromolecules **28**, 6754 (1995).